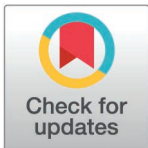


RESEARCH ARTICLE

VAPA mediates lipid exchange between *Leishmania amazonensis* and host macrophages

Ilona Gdovinova^{1,2}, Albert Descoteaux^{1,2*}**1** INRS- Centre Armand-Frappier Santé Biotechnologie, Laval, Québec, Canada, **2** Infectiopôle INRS, Laval, Québec, Canada* albert.descoteaux@inrs.ca

Abstract

Leishmania is a vacuolar pathogen that replicates within parasitophorous vacuoles inside host phagocytes. To promote its replication, *Leishmania* relies on a panoply of strategies to acquire macromolecules such as lipids from host macrophages. In this study, we have evaluated the role of VAPA, an endoplasmic reticulum-resident membrane protein involved in inter-organellar lipid transport, in macrophages infected with *L. amazonensis*. Following infection of bone marrow-derived macrophages with *L. amazonensis* metacyclic promastigotes, we observed that VAPA gradually associates with communal parasitophorous vacuoles. Knockdown of VAPA prevented the replication of *L. amazonensis*, which was accompanied by an impaired parasitophorous vacuole expansion. Using fluorescent ceramide, we established that VAPA is required for the transport of sphingolipids to the parasitophorous vacuoles and for its acquisition by *L. amazonensis* amastigotes. Proximity-ligation assays revealed that *L. amazonensis* hijacks VAPA by disrupting its interactions with the host cell lipid transfer proteins CERT and ORP1L. Finally, we found that VAPA is essential for the transfer of the *Leishmania* virulence glycolipid lipophosphoglycan from the parasitophorous vacuoles to the host cell endoplasmic reticulum. We propose that VAPA contributes to the ability of *L. amazonensis* to colonize macrophages by mediating bi-directional transfer of lipids essential for parasite replication and virulence between the parasitophorous vacuoles and the host cell endoplasmic reticulum.

OPEN ACCESS

Citation: Gdovinova I, Descoteaux A (2025) VAPA mediates lipid exchange between *Leishmania amazonensis* and host macrophages. PLoS Pathog 21(3): e1012636. <https://doi.org/10.1371/journal.ppat.1012636>

Editor: Dawn M Wetzel, UT Southwestern: The University of Texas Southwestern Medical Center, UNITED STATES OF AMERICA

Received: October 1, 2024

Accepted: March 3, 2025

Published: March 31, 2025

Copyright: © 2025 Gdovinova, Descoteaux. This is an open access article distributed under the terms of the [Creative Commons Attribution License](https://creativecommons.org/licenses/by/4.0/), which permits unrestricted use, distribution, and reproduction in any medium, provided the original author and source are credited.

Data availability statement: All relevant data are within the manuscript and its [Supporting Information](#) files.

Funding: This work was supported by Canadian Institutes of Health Research (www.cihr-irsc.gc.ca) grants PJT-156416 and PJT-186114 to AD. The funders had no role in study design,

Author summary

The protozoan parasite *Leishmania amazonensis* replicates in macrophages, within communal parasitophorous vacuoles. To satisfy its various auxotrophies, this parasite must obtain macronutrients and metabolites from its host cell, including lipids. To salvage host sphingolipids, we obtained evidence that *L. amazonensis* exploits a macrophage nonvesicular lipid transport mechanism that requires the endoplasmic reticulum membrane protein VAPA. Moreover, we found that VAPA is also required for the transfer of the *Leishmania* virulence glycolipid lipophosphoglycan from the parasitophorous vacuole to the macrophage endoplasmic reticulum. The fact that VAPA is essential for *L. amazonensis*

data collection and analysis, decision to publish, or preparation of the manuscript.

Competing interests: I have read the journal's policy and the authors of this manuscript have the following competing interests: AD is the holder of the Canada Research Chair on the Biology of intracellular parasitism.

to colonize macrophages is consistent with the central role that VAPA plays in mediating bi-directional transfer of lipids and illustrates the importance of the host cell endoplasmic reticulum in this host-parasite interaction.

Introduction

The protozoan parasite *Leishmania* is a vacuolar pathogen responsible for the leishmaniasis, a spectrum of human diseases ranging from a confined cutaneous lesion to a progressive visceral infection that can be fatal if left untreated [1]. Following inoculation into a mammalian host by an infected sand fly, infectious promastigote forms of the parasite are taken up by phagocytes. Internalized promastigotes evade microbicidal mechanisms associated to phagocytosis by subverting phagolysosomal biogenesis to generate parasitophorous vacuoles (PVs) in which they differentiate and replicate as mammalian stage amastigotes [2–9]. To obtain the membrane required for expansion and maintenance of those PVs, *Leishmania* modulates their interactions with trafficking vesicles and sub-cellular compartments by hijacking the host cell membrane fusion machinery [10–16]. Hence, knockdown or deletion of host cell soluble *N*-ethylmaleimide-sensitive factor attachment protein receptors (SNAREs) associated to the endoplasmic reticulum (ER) and to endosomes inhibited parasite replication and PV enlargement [10,14,17].

Leishmania displays various auxotrophies and must therefore acquire essential host-derived nutrients and macromolecules to promote its replication [18–20]. In this context, lipid metabolism in *Leishmania* is of interest as it differs from that in mammalian cells and may be exploited for the development of novel therapeutic approaches [21,22]. Hence, in contrast to insect stage promastigotes which rely on *de novo* synthesis to produce the majority of their lipids, amastigotes acquire most of their lipids from the mammalian host [23]. In the case of sphingolipids, evidence that *de novo* synthesis is unnecessary for the proliferation of intramacrophage amastigotes arose from the observation that *L. major* mutants defective in ceramide and sphingolipid biosynthesis were fully infective in an experimental model of cutaneous leishmaniasis [24,25]. Rather, *Leishmania* amastigotes acquire and remodel host sphingolipids, which contributes to their ability to colonize macrophages [26]. However, the mechanism by which amastigotes salvage mammalian host sphingolipids remains to be elucidated.

In mammalian cells the ER is the site of *de novo* synthesis of ceramide, the precursor of most sphingolipids [27]. Ceramide is transported to the Golgi where it is converted to sphingomyelin and other complex sphingolipids [28]. Transfer of ceramide from the ER to the Golgi is mediated by the ceramide transport protein CERT which associates with the ER-resident membrane protein VAMP-associated proteins (VAPs) [29]. Those proteins are components of membrane contact sites (MCS), which are regions of close contact between organelles specialized in the non-vesicular trafficking of molecules such as lipids and ions between organelles [30–32]. In recent years, MCS components were shown to be hijacked by vacuolar pathogens to establish MCS between pathogen-containing vacuoles and host cell organelles, as a strategy to promote their intracellular replication [33–36]. One example is the bacterial pathogen *Chlamydia trachomatis*, which through the action of secreted effectors recruits CERT and other host factors to the inclusion and brings the ER in close proximity [37–39]. Through interactions with VAPA/B, *C. trachomatis* then reroutes sphingolipid biosynthesis to its replicative niche [38,40]. Given the importance of the ER in the synthesis and inter-organelle trafficking of lipids, we explored the role of VAPA in the context of *L. amazonensis*-infected macrophages. Our findings indicate that *L. amazonensis* amastigotes exploits VAPA to promote their replication through the bi-directional exchange of lipids

essential for parasite replication and virulence. This study highlights the importance of the host cell ER for the intracellular replication of *L. amazonensis*.

Results

The ER protein VAPA associates with *L. amazonensis*-harboring communal parasitophorous vacuoles

Previous studies revealed that *L. amazonensis*-harboring communal PVs are hybrid compartments composed of both host ER and endocytic pathway components [10,41]. Those PVs acquire ER content and membrane components through continuous interactions with this organelle [41]. The protein VAPA is a prominent ER membrane tether involved in the interactions and lipid transfer between the ER and other organelles through the formation of MCS [42]. To investigate the potential role of VAPA in the intracellular fate of *L. amazonensis*, we first determined the kinetics of its association with PVs. To this end, we infected bone marrow-derived macrophages (BMM) with *L. amazonensis* metacyclic promastigotes and we used confocal immunofluorescence microscopy to assess the fate of VAPA at various time points post-phagocytosis. As controls, we infected BMM with *L. major* metacyclic promastigotes, which differentiate and replicate as amastigotes in tight-fitting individual PVs and we also fed BMM with serum-opsonized zymosan. As illustrated in Fig 1A and 1B we found that VAPA accumulates on communal PVs containing *L. amazonensis* amastigotes starting at 24 h post-phagocytosis. In contrast, we observed that VAPA was associated with a significantly smaller subset of PVs harboring *L. major* amastigotes and of phagosomes containing zymosan. Distribution of VAPA in uninfected BMM is shown in Fig 1A. Western blot analysis revealed no variations in VAPA levels in *L. amazonensis*-infected BMM over a 72 h post-infection kinetics (Fig 1D). To provide further evidence that VAPA associates with the membrane of communal PVs, we assessed its colocalization with LAMP1 which is also recruited to these PVs. As shown in Fig 1C, VAPA colocalizes with LAMP1 at the PV membrane. These results indicate that VAPA associates with communal PVs containing *L. amazonensis* amastigotes and raise the possibility that it contributes to their development.

VAPA contributes to the replication of *L. amazonensis* and PV expansion

Given the association of VAPA with communal PVs, we sought to investigate its role in the development of those compartments and on the intracellular fate of *L. amazonensis*. We infected BMM (untreated or treated with either siRNA to VAPA or scrambled siRNA) with *L. amazonensis* metacyclic promastigotes and at various time points post-infection we assessed parasite burden and PV surface area. We included BMM infected with *L. major* metacyclic promastigotes in our analyses. As depicted in Fig 2A, whereas VAPA knockdown had no impact on the phagocytosis of *L. amazonensis*, it severely restricted parasite replication. In the case of *L. major*, we noticed a slight reduction in its replication in VAPA knockdown BMM at 24 h and 48 h post-infection and at 72 h post-infection we did not detect a significant impact of VAPA knockdown on parasite replication (Fig 2B). To further confirm that VAPA is required for the replication of *L. amazonensis*, we measured BrdU incorporation by intracellular parasites [43]. BMM (untreated or treated with siRNA to VAPA or with scrambled siRNA) were infected with *L. amazonensis* metacyclic promastigotes and were incubated in the presence of BrdU for up to 72 h post-infection. As shown in Fig 2C and 2D, BrdU incorporation by *L. amazonensis* was significantly lower in BMM treated with siRNA to VAPA compared to untreated BMM or BMM treated with scrambled siRNA, consistent with an inhibition of parasite replication. The inability of *L. amazonensis* to replicate in VAPA knockdown BMM correlated with smaller PVs size at 48 h and 72 h post-infection (Fig 2E). These results indicate

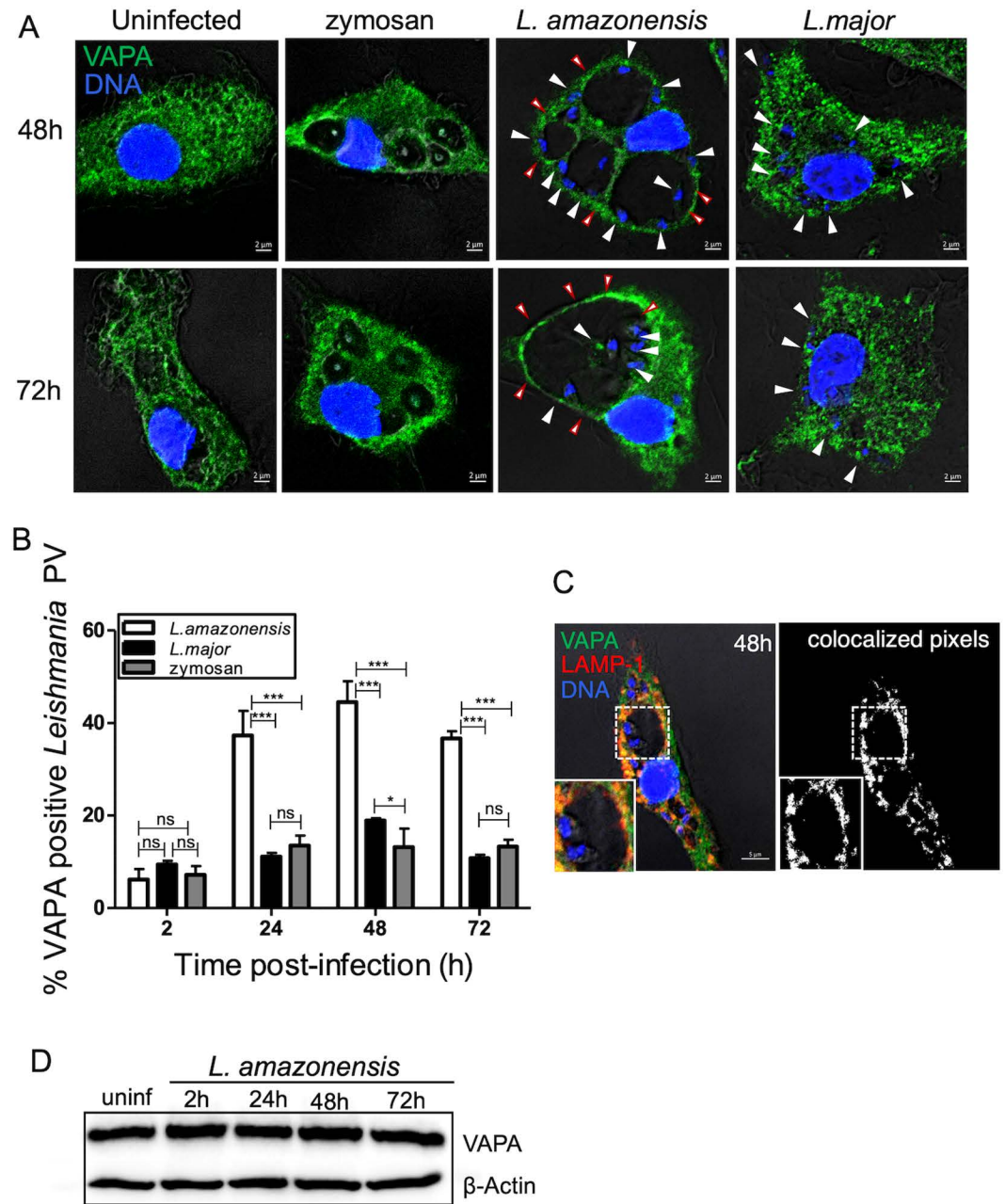


Fig 1. VAPA associates with *L. amazonensis*-harboring communal PVs. BMM were infected with *L. amazonensis* or *L. major* metacyclic promastigotes for the indicated time points. Controls consisted of untreated BMM and BMM fed with zymosan. (A) Distribution of VAPA (green) and its association with PVs were assessed by confocal immunofluorescence microscopy. DNA is shown in blue. (B) Quantification of the association of VAPA to *L. amazonensis*- and *L. major*-harboring PVs and to zymosan-containing phagosomes. (C) Colocalization of LAMP1 with VAPA on communal PVs harboring *L. amazonensis* at 48 h post-infection. Colocalization (white pixels) of LAMP-1 (red) with VAPA (green) was assessed and quantified by confocal immunofluorescence microscopy. Insets display the PV area. DNA is shown in blue. (D) Western blot analysis of VAPA levels over time in *L. amazonensis*-infected BMM. Data are presented as the means \pm standard errors of the means (SEM) of values from three independent experiments. White arrowheads denote internalized parasites. Representative images from three experiments are shown. **, $P \leq 0.01$; ***, $P \leq 0.001$.

<https://doi.org/10.1371/journal.ppat.1012636.g001>

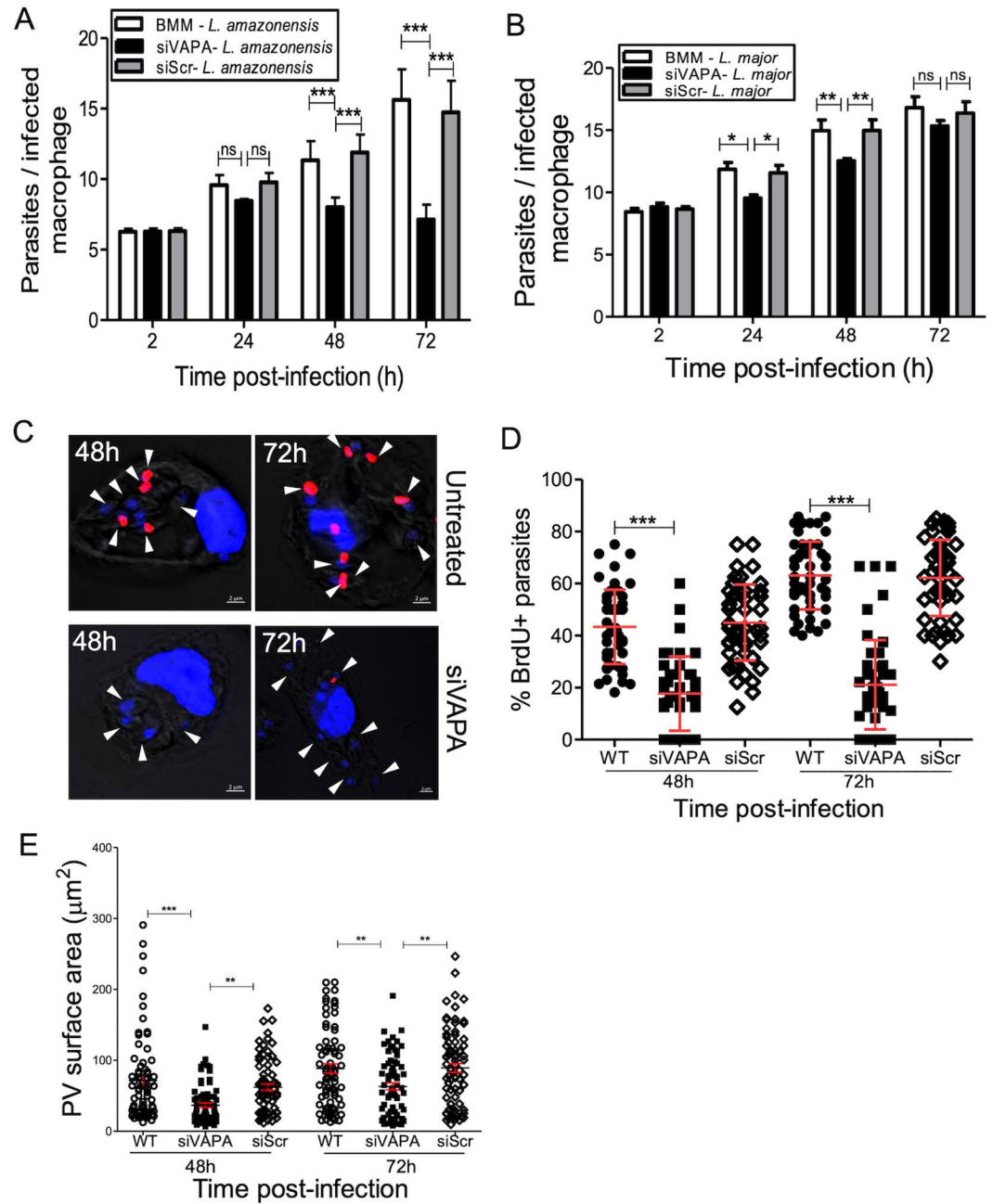


Fig 2. VAPA regulates the replication of *L. amazonensis* and PV expansion. BMM (untreated, treated with siRNA to VAPA, or treated with scrambled siRNA) were infected with *L. amazonensis* or *L. major* metacyclic promastigotes and at various time points post-phagocytosis parasite replication and PV size were assessed. (A) Quantification of *L. amazonensis* parasite burden at 2, 24, 48, and 72 h post-infection. Data are presented as the means \pm SEM of values from three independent experiments. **, $P \leq 0.01$; ***, $P \leq 0.001$. (B) Quantification of *L. major* parasite burden at 2, 24, 48, and 72 h post-infection. Data are presented as the means \pm SEM of values from three independent experiments. *, $P \leq 0.05$; **, $P \leq 0.01$. (C) Labeling of *L. amazonensis* amastigotes with BrdU in BMM (untreated or treated with siRNA to VAPA) infected for 48 h and 72 h. (D) Percent of BrdU+ parasites in BMM (untreated, treated with siRNA to VAPA or with scrambled siRNA) at 48 h and 72 h post-phagocytosis. Data are presented as the means \pm SEM of values from three independent experiments. ***, $P \leq 0.001$. (E) Quantification of PV size in BMM infected with *L. amazonensis* at 48 and 72 h post-phagocytosis. Data are presented as a cloud with means \pm standard deviations (SD) of values from three independent experiments for a total of 450 PVs. **, $P \leq 0.01$; ***, $P \leq 0.001$. Blots showing the efficacy the siRNA-mediated VAPA knockdowns are shown in [S1 Fig](#).

<https://doi.org/10.1371/journal.ppat.1012636.g002>

a role for VAPA in the replication of *L. amazonensis* amastigotes and in communal PV expansion.

Acquisition of sphingolipids by *L. amazonensis* requires VAPA

Leishmania amastigotes salvage most of their lipids, including sphingolipids, from the host [23,25]. Since VAPA is involved in the transfer of lipids synthesized in the ER to their destination organelle [44], we assessed whether it mediates the transfer of ceramide/sphingolipids to the PVs. To this end, BMM (untreated, treated with either siRNA to VAPA or scrambled siRNA, or mock lipofected) infected for 48 h with *L. amazonensis* metacyclic promastigotes were labeled with fluorescent ceramide (BODIPY FL C5-Ceramide). Using live cell imaging, we observed incorporation of fluorescent sphingolipids into *L. amazonensis* amastigotes present within PVs in control groups (Fig 3A and 3B). In contrast, *L. amazonensis* amastigotes did not acquire fluorescent sphingolipids in VAPA knockdown BMM, consistent with a role for VAPA in the acquisition of host sphingolipids by *L. amazonensis*. VAPA was previously shown to be involved in the transfer of ceramide/sphingolipids to the *Chlamydia* inclusion through interactions with the ceramide transfer protein CERT [37,38]. We therefore sought to determine whether VAPA associates with CERT and contributes to the acquisition of ceramide/sphingolipids by *L. amazonensis*. We included as a control the endosomal/lysosomal oxysterol lipid binding protein ORP1L which also associates with VAPA [45]. Generation of ceramide is notably mediated by the enzymatic activity of neutral sphingomyelinase 2 (nSMase2), which closely associates with the ER [46]. We assessed its localization in infected BMM and we used zymosan as a control. At 72 h post-phagocytosis of *L. amazonensis* metacyclic promastigotes, we found that labeling for CERT and to a lesser extent ORP1L and nSMase2, was more intense around communal PVs. Whereas CERT colocalized with VAPA at PVs, we observed little colocalization of ORP1L and nSMase2 with VAPA (Fig 4A-C). Given that both CERT and ORP1L are binding partners of VAPA and associate with *L. amazonensis*-harboring PVs, we next assessed the potential role of CERT and ORP1L on the replication of *L. amazonensis* and on PV size. As illustrated in Fig 4D and 4E, CERT knockdown had a minimal impact on the replication of *L. amazonensis* but resulted in a reduced PV size. In contrast, ORP1L knockdown resulted in increased parasitemia despite a defect in PV expansion (Fig 4F and 4G).

L. amazonensis disrupts VAPA-CERT and VAPA-ORP1L complexes

In the context of membrane contact sites, co-localization by immunofluorescence confocal microscopy may not be sufficient to conclude that VAPA forms complexes with CERT and ORP1L. We therefore used proximity ligation assay (PLA) to assess *in situ* VAPA-CERT and VAPA-ORP1L protein-protein interactions in uninfected BMM and in BMM infected with *L. amazonensis* metacyclic promastigotes for 24 h, 48 h, and 72 h. With PLA, proximity between two proteins (below 40 nm) is detected by fluorescent dots. As shown in Fig 5A-D, VAPA forms complexes with CERT and ORP1L in uninfected BMM. Remarkably, both VAPA-CERT and VAPA-ORP1L *in situ* complexes disappeared within 6 h post-infection in infected BMM. Disruption of VAPA-lipid transfer protein complexes by *L. amazonensis* was also observed for VAPA-GLTP (glycolipid transfer protein) *in situ* complexes (S4 Fig), indicating that *L. amazonensis* efficiently disrupts interactions of VAPA with lipid transfer proteins. Previous studies revealed that insertion of the *Leishmania* pathogenicity glycolipid LPG into host cell membranes disrupts lipid microdomains, thereby altering protein distribution [7,47,48]. Similarly, the *Leishmania* surface metalloprotease GP63 targets and cleaves a subset of host cell proteins, which may affect protein complex formation [49]. To investigate the possibility that either LPG or GP63 are involved in the disruption of *in situ* VAPA-ORP1L complexes, we

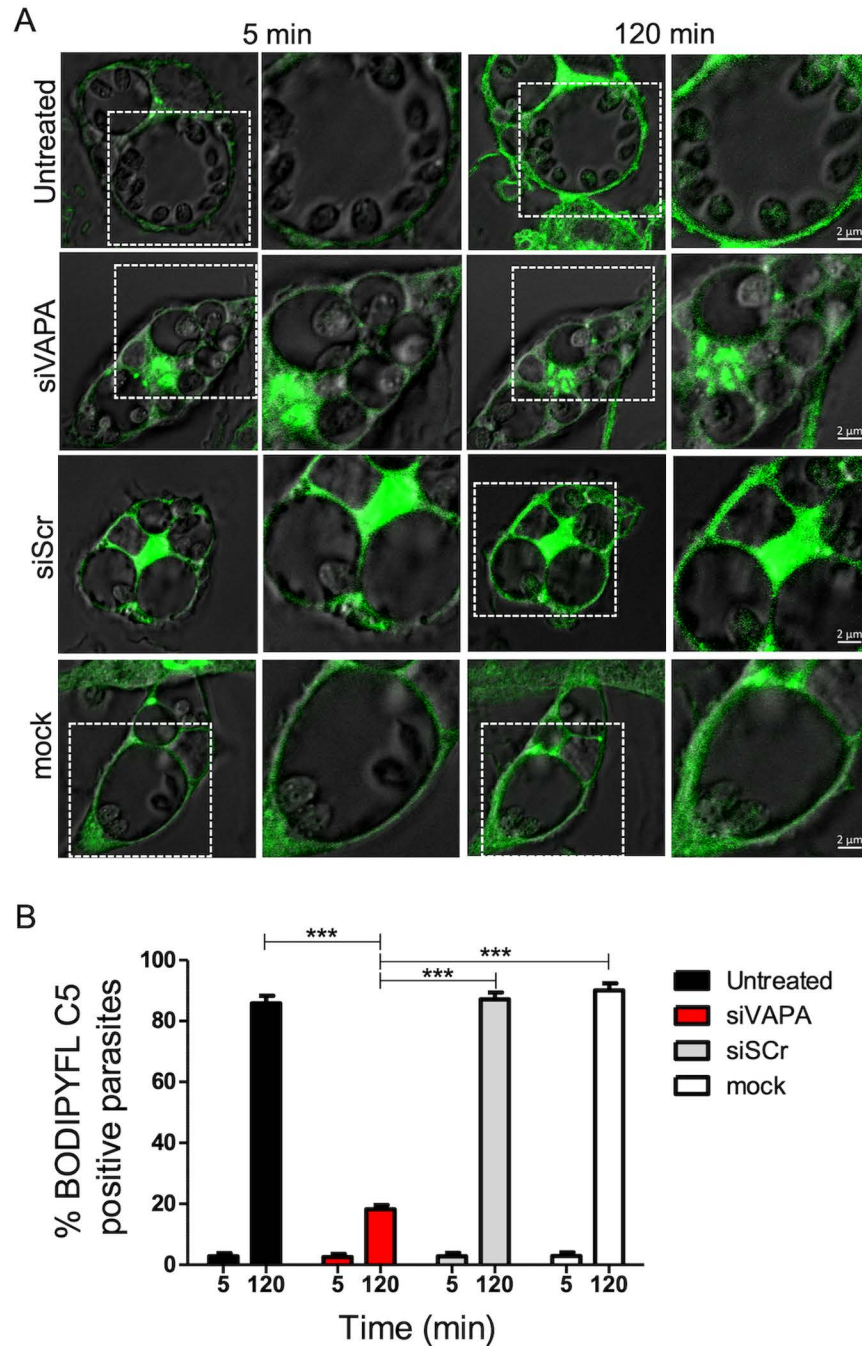


Fig 3. VAPA is required for the acquisition of sphingolipids by *L. amazonensis*. BMM (untreated, treated with siRNA to VAPA, treated with scrambled siRNA, and mock transfected) were infected with *L. amazonensis* metacyclic promastigotes and at 48h post-infection BMM were incubated with BODIPY FL C5-Ceramide (green). (A) Images of live cells were acquired at 5 min and 120 min after the addition of BODIPY FL C5-Ceramide. (B) Quantification of BODIPYFL-C5 positive *L. amazonensis* amastigotes at 5 min and 120 min after the addition of BODIPY FL-C5-Ceramide. Data are presented with means \pm standard deviations (SD) of values from three independent experiments. ***, $P \leq 0.001$ (in comparison to controls, siScr and mock). Blots showing the efficacy the siRNA-mediated VAPA knockdowns are shown in S1 Fig.

<https://doi.org/10.1371/journal.ppat.1012636.g003>

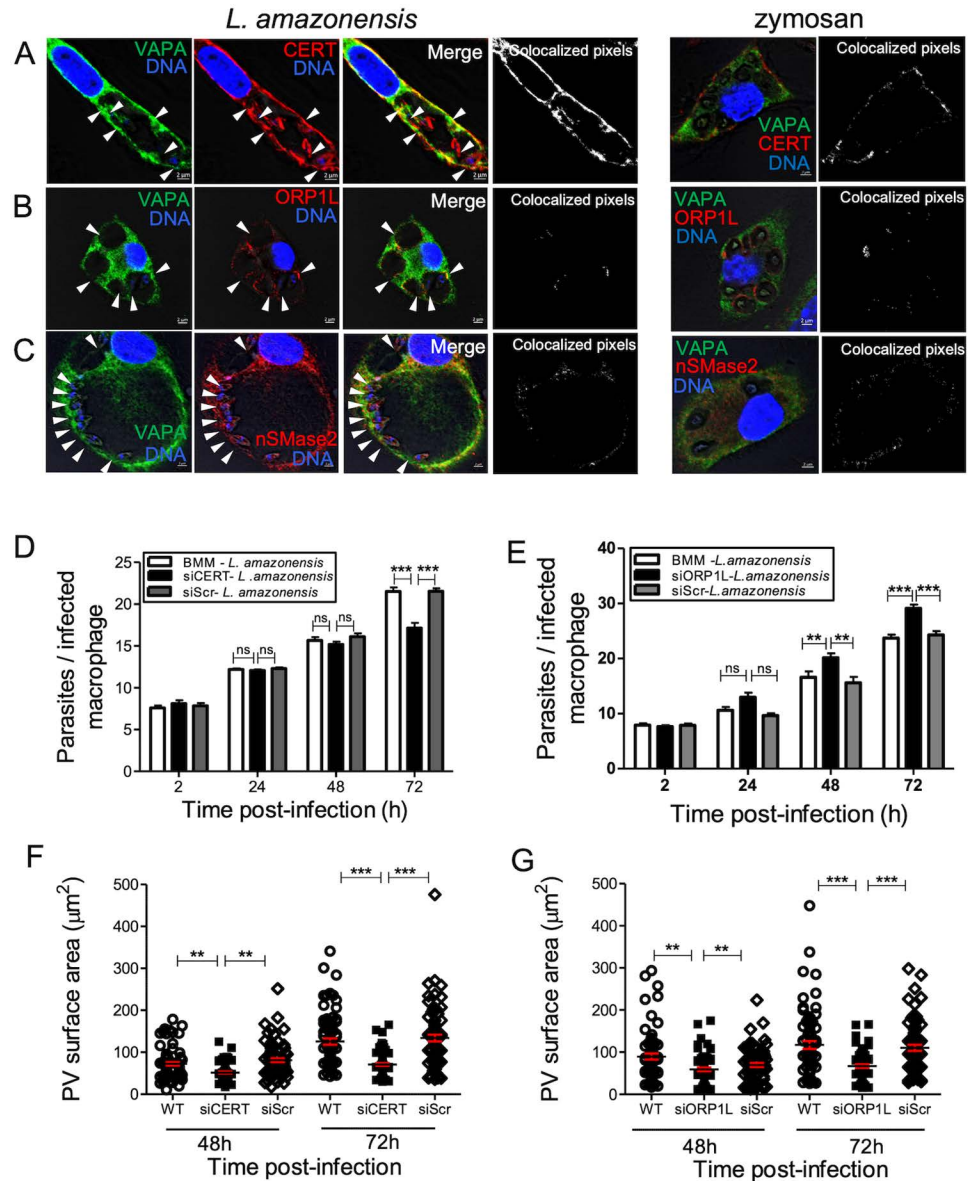


Fig 4. CERT and ORP1L associate with *L. amazonensis*-harboring communal PVs and regulate their expansion. BMM were infected with *L. amazonensis* metacyclic promastigotes and at the indicated time points the localization of CERT (red) (A) and ORP1L (red) (B) was assessed by immunofluorescence confocal microscopy. Co-localization of VAPA (green) with CERT (red) (A) and ORP1L (red) (B) was assessed by immunofluorescence confocal microscopy at 72 h post-infection. DNA is shown in blue. White arrowheads denote internalized parasites. Representative images from three independent experiments are shown. BMM (normal, treated with siRNA to CERT or scramble siRNA) were infected with *L. amazonensis* metacyclic promastigotes and at the indicated time points post-infection, parasite burden (C) and PV size (D) were assessed. BMM (untreated, treated with siRNA to ORP1L or scramble siRNA) were infected with *L. amazonensis* metacyclic promastigotes and at the indicated time points post-infection parasite burden (E) and PV size (F) were assessed. Data are presented as the means \pm SD of values from three independent experiments. **, $P \leq 0.01$; ***, $P \leq 0.001$. For the determination of PV surface area (D, F) data are presented as clouds with means \pm SD of values from three independent experiments for a total of 450 PVs. **, $P \leq 0.01$; ***, $P \leq 0.001$. Blots showing the efficacy the siRNA-mediated CERT and ORP1L knockdowns are shown in S2 Fig.

<https://doi.org/10.1371/journal.ppat.1012636.g004>

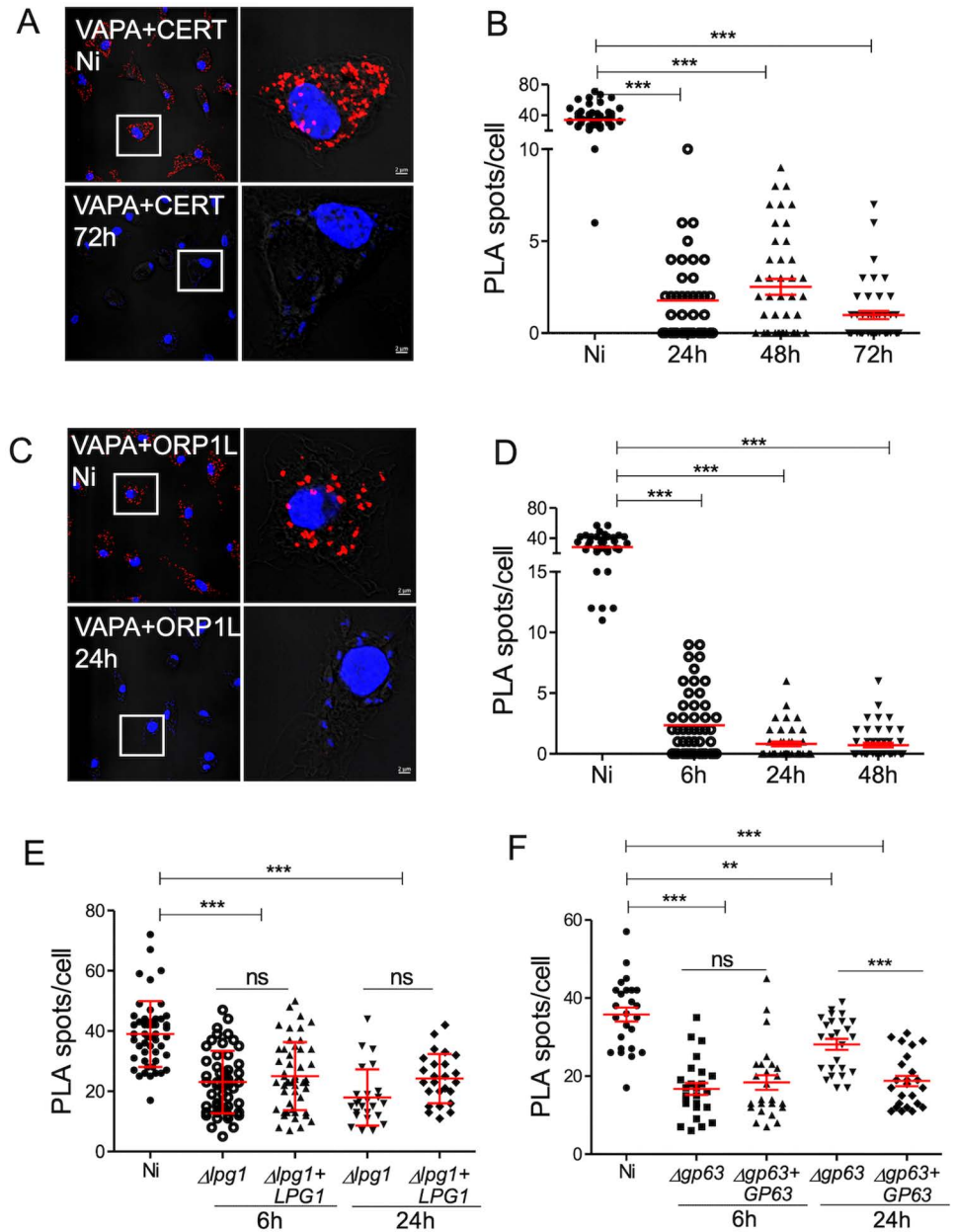


Fig 5. *L. amazonensis* hijacks VAPA. BMMs were infected or not with either *L. amazonensis* (A-D), $\Delta lpg1$ and $\Delta lpg1 + LPG1$ *L. donovani* (E) or $\Delta gp63$ and $\Delta gp63 + GP63$ *L. major* (F) metacyclic promastigotes. At the indicated time points post-infection, *in situ* VAPA-CERT (A) and VAPA-ORP1L (C) complexes were detected by proximity ligation and visualized by confocal immunofluorescence microscopy (red dots). DNA is in blue. Representative images from 3 independent experiments are shown. Quantification of *in situ* complexes for VAPA-CERT (B) and VAPA-ORP1L (D) in uninfected BMM and in BMM infected with *L. amazonensis*. Quantification of *in situ* complexes for VAPA-ORP1L in uninfected BMM and in BMM infected with either (E) $\Delta lpg1$ and $\Delta lpg1 + LPG1$ *L. donovani* or (F) $\Delta gp63$ and $\Delta gp63 + GP63$ *L. major*. Data are presented as clouds with means \pm standard deviations (SD) of values from three independent experiments for a total of 75 cells in each group. **, $P \leq 0.01$; ***, $P \leq 0.001$. Controls for the proximity ligation assays are shown in S3 Fig.

<https://doi.org/10.1371/journal.ppat.1012636.g005>

infected BMM with $\Delta lpg1$ and $\Delta lpg1+LPG1$ *L. donovani* and with $\Delta gp63$ and $\Delta gp63+GP63$ *L. major* metacyclic promastigotes. At 6 h and 24 h post-infection, we assessed VAPA-ORP1L *in situ* interactions through PLA. VAPA-ORP1L complexes were disrupted at 6 h post-infection regardless of the presence or absence of LPG and GP63 (Fig 5E and 5F). We noted that infection of BMM with *L. major* and *L. donovani*, which replicate in tight-fitting individual PVs, did not fully disrupt VAPA-ORP1L complexes as observed with *L. amazonensis*. At 24 h post-infection, we observed a significant increase in the number of VAPA-ORP1L *in situ* complexes in BMM infected with the $\Delta gp63$ *L. major* mutant with respect to 6 h post-infection time point (Fig 5F). These results suggest that *L. amazonensis* hijacks VAPA and that neither LPG nor GP63 are responsible for the disruption of VAPA-CERT and VAPA-ORP1L. GP63 might however play a role in preventing the formation of those complexes at later time point post-infection.

VAPA is required for the transfer of LPG out of the PV

LPG, the major lipid component of the *Leishmania* promastigote surface coat [50], is released from the parasite following phagocytosis and redistributes to the ER of infected macrophages [51]. We previously reported that trafficking out of the PVs of this *Leishmania* virulence glycolipid requires the SNAREs Sec22b and syntaxin-5, which regulate ER-Golgi trafficking [51]. Given that VAPA participates in multiple lipid transport pathways from the ER to destination organelles [44,52], we investigated the possibility that this protein contributes to the transfer of LPG from the PV to the ER. First, we infected BMM with *L. major* metacyclic promastigotes and at 6 h post-phagocytosis, we analyzed the distribution of LPG with respect to VAPA by confocal immunofluorescence microscopy. We used *L. major* instead of *L. amazonensis* because the anti-LPG antibody CA7AE recognizes more efficiently *L. major* LPG. As shown in Fig 6A, LPG released by *L. major* promastigotes co-localized with VAPA, suggesting a possible interaction between these two molecules. Next, we infected BMM (untreated, treated with either siRNA to VAPA or scrambled siRNA, mock transfected) with *L. major* metacyclic promastigotes and at 6 h post-phagocytosis we assessed the distribution of LPG. The distribution of LPG within infected BMM was strikingly altered in the absence of VAPA, as depicted in Fig 6B. Hence, whereas LPG was evenly distributed throughout control infected BMM, it was confined to the cell periphery in VAPA knockdown BMM. Further analysis indicated that in control infected BMM, LPG was present in the ER as determined by its colocalization with the ER marker ERseeing as well as with endosomes/lysosomes, as it co-localized with LAMP1 (Fig 6C). In the absence of VAPA, LPG predominantly co-localized with LAMP1, indicating its presence within late endosomes/lysosomes (Fig 6C). These results indicate that VAPA is involved in the transport of LPG from the PVs to the host cell ER and suggest that it can mediate bi-directional lipid transport.

Discussion

Vacuolar pathogens scavenge macromolecules, nutrients and metabolites from their host cell. To this end, they establish communication between the vacuole in which they replicate and host cell organelles [33,35,36]. In the present study, we investigated the role of the macrophage ER membrane protein VAPA in the interaction between *L. amazonensis* and its host cell. We found that VAPA is essential for *L. amazonensis* replication and PV expansion as well as for the acquisition of sphingolipids by the parasite. Moreover, we found that VAPA is essential for the transfer of the virulence glycolipid LPG from the PV to the host cell ER, indicating that VAPA mediates bi-directional lipid transport (Fig 7).

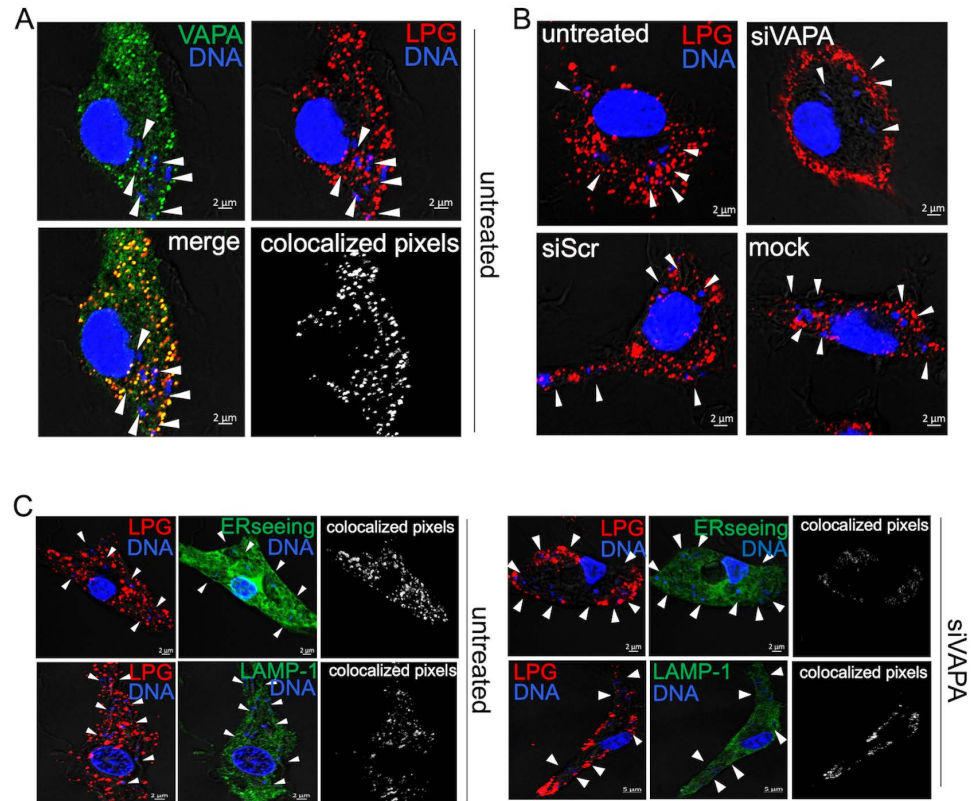


Fig 6. VAPA is required for the transfer of LPG to the host cell ER. (A) BMM were infected with *L. major* metacyclic promastigotes and at 6 h post-phagocytosis, the localization of VAPA (green) and LPG (red) were assessed by confocal immunofluorescence microscopy. Colocalized pixels are in white and DNA is in blue. (B) BMM (untreated or treated with siRNA to VAPA, scrambled siRNA, or mock transfected) were infected with *L. major* metacyclic promastigotes and at 6 h post-phagocytosis, the localization of LPG (red) was assessed by confocal immunofluorescence microscopy. DNA is in blue. (C) Untreated BMM (left panel) or BMM treated with siRNA to VAPA (right panel) were infected with *L. major* metacyclic promastigotes and at 6 h post-phagocytosis, the co-localization of LPG (red) with ERSeeing (green) or LAMP1 (green) was assessed by confocal immunofluorescence microscopy. Colocalized pixels are in white, DNA is in blue. White arrowheads denote internalized parasites. Representative images from 3 independent experiments are shown. Blots showing the efficacy of the siRNA-mediated VAPA knockdowns are shown in S1 Fig.

<https://doi.org/10.1371/journal.ppat.1012636.g006>

The vast majority of a cell's organelles are connected to the ER through MCS, forming a network through which lipids, ions, and metabolites are travelling [30,32,53,54]. Our finding that VAPA accumulates around *L. amazonensis*-harboring PVs indicated that these PVs are connected through the ER to the host cell organelle network. Hence, one can envision that integration of *L. amazonensis*-harboring PVs in this ER-orchestrated organelle network facilitates the acquisition of host molecules by the parasite as well as the release of *Leishmania* molecules into the organelle network, and that these exchanges of molecules are essential for the ability of *L. amazonensis* to colonize macrophages. The observation that VAPA is required for the replication of *L. amazonensis* and for PV expansion supports the notion that contact between PVs and the ER plays a central role in the pathogenesis of *Leishmania* and is in agreement with a key role for the ER in this host-pathogen interaction [15,41]. It is also consistent with the notion that VAPA contributes to the replication of *Leishmania* by regulating the transfer of lipids from the ER to the PV.

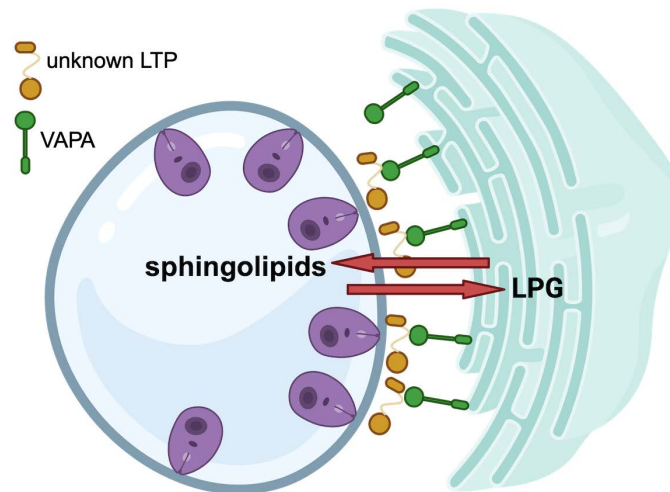


Fig 7. Proposed model for the role of VAPA in macrophages infected with *L. amazonensis*. VAPA is required for the acquisition of host sphingolipids by *L. amazonensis* amastigotes, as well as for the transfer of the *Leishmania* virulence glycolipid lipophosphoglycan (LPG) to the host cell endoplasmic reticulum. The identity of the lipid transfer protein(s) (LTP) involved in this bi-directional lipid transfer remains to be determined. Created with BioRender.

<https://doi.org/10.1371/journal.ppat.1012636.g007>

In contrast to promastigotes, amastigotes are unable of *de novo* synthesis for most lipids and therefore rely on the salvage and remodeling of host lipids to satisfy their lipid requirements [23,25]. In spite the fact that recent studies have investigated how *Leishmania* acquires host lipids, the underlying mechanisms remain poorly understood. Hence, a study on the role of the V-ATPase subunit ATP6V₀d2 in the biogenesis of *L. amazonensis*-harboring PVs revealed its importance in PV enlargement [55]. The authors of that study proposed that ATP6V₀d2 participates in cholesterol influx, impacting the biogenesis of host cell membranes and PV formation [55], but cholesterol uptake by *L. amazonensis* was not directly evaluated. The discovery that the scavenger receptor CD36, a fatty acid transporter [56], accumulates on expanding PVs containing *L. amazonensis* and is required for parasite growth and PV expansion led the authors to suggest that CD36 may function as a channel to exchange lipids to and/or from the PV [57]. In this regard, a potential source of fatty acids are lipid bodies (LBs), which accumulate in close proximity of PVs in *Leishmania*-infected macrophages [58,59]. Interestingly, a recent study shed light on how *L. donovani* may exploit LBs to acquire fatty acids [60]. It was shown that biogenesis of LBs and their recruitment to *L. donovani*-containing PVs is mediated by Rab18 and TRAPPC9. Furthermore, the authors provided evidence that fluorescently-labelled fatty acids present in LBs were recruited in/on PVs containing *L. donovani* [60], suggesting that this parasite acquires fatty acids from PV-associated LBs. There was however no evidence in that study indicating that fluorescent fatty acids are incorporated by *Leishmania*. Sphingolipids received a particular attention as they are acquired and remodeled at high levels by *Leishmania* amastigotes [25] and are likely to play a key role in virulence [21,23,26,61,62]. However, the mechanism by which *Leishmania* salvages sphingolipids remains elusive [23]. Our results obtained using BODIPY FL C5-Ceramide add novel insight into this process, with VAPA being essential for the acquisition of fluorescent sphingolipids by *L. amazonensis* present in communal PVs. This approach has some limitations, since the use of BODIPY FL C5-Ceramide is not quantitative and it is not possible to determine the modifications that may have occurred in infected macrophages. The identity of the fluorescent sphingolipid(s) detected in *L. amazonensis* therefore remains to be established. Given

the importance of sphingolipids in cellular functions [63] and the essential role of VAPA in their acquisition by *L. amazonensis* amastigotes, it is reasonable to propose that the defect in parasite replication and PV expansion in the absence of VAPA is related to some extent to the inability to salvage host sphingolipids. A better understanding of how VAPA contributes to the acquisition of sphingolipids by *L. amazonensis* will be necessary to develop novel therapeutic approaches to interfere with the transfer of host sphingolipids to *Leishmania*.

The surface glycolipid LPG [50] plays a central role during the life cycle of *Leishmania*, as it contributes to the colonization of both the sand fly vector and the mammalian host [64–66]. In macrophages, LPG enables *Leishmania* to interfere with signalling pathways [3,67,68], to inhibit phagolysosomal biogenesis [2,4,7], to activate the inflammasome [69], and to alter mitochondrial biology [70]. To exert its action, LPG must notably exit the PV and redistribute within infected macrophages. We recently reported that upon phagocytosis, LPG is transported beyond the PV into the host cell ER and ERGIC via a mechanism dependent on the SNAREs Sec22b and syntaxin-5 [51]. These findings are consistent with the notion that vesicular trafficking plays an important role in the spread of LPG inside infected macrophages. Interestingly, our results suggest that direct interaction between the PV and the ER through VAPA may also play a role in the transfer of LPG between these two organelles. Whether the Sec22b-dependent and the VAPA-dependent mechanisms involved in the transfer of LPG from the PV to the ER are part of the same pathway or represent two distinct pathways is not known. Interestingly, it has been reported that VAPA binds to and colocalizes with several SNAREs, including rsec22, the rat homologue of yeast sec22p [71]. In yeast, Sec22 was shown to interact with lipid transfer proteins, and inhibition of Sec22 leads to defects in lipid metabolism at contact sites between the ER and plasma membrane [72]. More recently, it was shown that Sec22b resides in phagosomal MCS where it acts as a tether at the ER-phagosome contacts and regulates phagosomal levels of phospholipids [73]. Clearly, additional studies will be required to further investigate the mechanism(s) by which VAPA and Sec22b contribute to the transfer of LPG from the PV to the host cell ER and to identify the putative lipid transfer protein involved in this process. Whereas the impact of LPG on macrophage functions has been well described, the consequences of its presence specifically within the host cell ER remain to be established. ER stress induced by pathological conditions have been associated to the activation of the NLRP3 inflammasome [74]. Previous work revealed that induction of ER stress in macrophages by *Leishmania* is associated with an increase survival of the parasite [75]. Whether LPG plays a role in this process is unknown. In this regard, activation of the NLRP3 inflammasome by *Leishmania* is mediated by LPG and it requires that LPG be delivered out the PV [69]. One may thus speculate that transfer of LPG from the PV to the host cell ER contributes to the ability of *Leishmania* to colonize macrophages, and that the impaired replication of *L. amazonensis* in VAPA knockdown macrophages may be in part related to the fact that LPG is not transferred to the ER. Future studies will be necessary to determine whether in addition to LPG, abundant glycolipids produced by *Leishmania* amastigotes such as glycoinositolphospholipids [76,77] traffick to the host cell ER and whether VAPA plays a role in this process.

Lipid transport from the ER to the destination organelles requires the interaction of VAPA with various lipid transfer proteins, including CERT and ORP1L [42,44]. Whereas we observed by confocal immunofluorescence microscopy the presence of CERT and to a lesser extent ORP1L on PVs and their partial co-localization with VAPA, proximity ligation assays revealed that *L. amazonensis* efficiently disrupts the VAPA-CERT and VAPA-ORP1L *in situ* complexes present in BMM. The use of a *L. donovani* mutant deficient in LPG and a *L. major* mutant deficient in GP63 allowed us to discard a role for these two major pathogenicity factors in the disruption of VAPA-ORP1L complexes. However, we noted an increase

in the number of those *in situ* complexes in the absence of GP63 at later time points post-infection, raising the possibility that GP63 plays a role in keeping VAPA from associating to ORP1L. Beyond the impact of GP63 on the VAPA-ORP1L *in situ* complexes observed at later time points post-infection, the mechanism by which interaction between VAPA and two prominent lipid transfer proteins is disrupted remains to be elucidated. Clearly, the rapid disruption of VAPA-CERT and VAPA-ORP1L complexes induced by *L. amazonensis* is consistent with a hijacking of VAPA by the parasite and raises the possibility that infection leads to the formation of novel VAPA-containing complexes which may contain proteins of either macrophage or parasite origin, or both. Such a scenario has been demonstrated in *Chlamydia*-infected cells where CERT is recruited to the *C. trachomatis* inclusion through interaction with the *Chlamydia* effector protein IncD [37]. In addition to the recruitment of CERT and VAPA to the inclusion, two host cell sphingomyelin synthases are recruited to the inclusion, leading to the generation of a sphingomyelin factory at the inclusion [38]. Whether VAPA forms complexes with a *Leishmania*-derived ceramide/sphingolipid transfer protein or associates with a sphingomyelin synthase as previously described for *Chlamydia* are issues that will deserve further investigation. The fact that the neutral sphingomyelinase 2 is present at the PV suggests that ceramide could be generated at this site but its fate remains unclear given that VAPA-CERT complexes are disrupted by *L. amazonensis*. Although our data suggest that CERT and ORP1L are not associated to VAPA in *L. amazonensis*-infected macrophages, we obtained evidence that both lipid transfer proteins play a role in the ability of *L. amazonensis* to replicate in macrophages. Hence, both CERT and ORP1L contribute to PV expansion, which may be related to the fact that sphingolipids and cholesterol are crucial components of cellular membranes [63,78]. It is also possible that absence of ORP1L results in the accumulation of damage to PV membrane, thereby preventing PV expansion [79]. The observation that knockdown of ORP1L led to an increased replication of *L. amazonensis* might be related to the fact that absence of ORP1L may favor the interaction of VAPA with another lipid transfer protein. In this regard, it is important to consider that in addition to VAPA, the VAP family includes VAPB, MOSPD1, MOSPD2, and MOSPD3 [42]. Over 250 human proteins were reported to interact with VAPA and VAPB and it was shown that these two VAPs share 50% of their interactomes [44], with the majority of these proteins being involved in lipid transfer between organelles [44]. The fact that VAPA knockdown is sufficient to inhibit *L. amazonensis* replication and acquisition of sphingolipids suggests that there is no functional redundancy at that level within the VAP family. Whether other VAP family members are involved in other aspects of the interaction between *Leishmania* and macrophages will deserve further investigation.

In sum, we have provided evidence that VAPA, a component of MCS involved in the transfer of lipids between the ER and other organelles [42,44], plays an important role in the ability of *L. amazonensis* to colonize macrophages. Integration of *L. amazonensis*-harboring communal PVs into the macrophage ER-orchestrated organelle network is consistent with the notion that the macrophage ER plays central role for the development of intracellular *Leishmania*.

Materials and methods

Ethic statement

Animal work was performed as stipulated by protocols 2112-01 and 2110-04, which were approved by the *Comité Institutionnel de Protection des Animaux* of the INRS-Centre Armand-Frappier Santé Biotechnologie. These protocols respect procedures on animal practice promulgated by the Canadian Council on Animal Care, described in the Guide to the Care and Use of Experimental Animals.

Bone marrow-derived macrophages

Bone marrow was extracted from the femurs and tibias of 8 to 12 week-old female and male 129/BL6 mice. BMMs were differentiated for 7 days in complete Dulbecco's modified Eagle's medium with glutamine (DMEM; Thermo Fisher Scientific) containing 10% heat-inactivated fetal bovine serum (FBS; HyClone), 10 mM HEPES, pH 7.4, penicillin (100 IU/mL) and streptomycin (100 µg/mL) and supplemented with 15% (vol/vol) L929 cell-conditioned medium as a source of colony-stimulating factor-1 (CSF-1), in a 37°C incubator with 5% CO₂. BMM were made quiescent by culturing them in DMEM without CSF-1 for 24 h prior to use.

Parasite culture and infection

The *Leishmania* strains used in this study were *L. amazonensis* LV79 strain (MPRO/BR/72/M1841, obtained from the American Type Culture Collection), *L. donovani* LV9 (MHOM/ET/67/Hu3:LV9) $\Delta lpg1$ mutant and its complemented counterpart $\Delta lpg1+LPG1$ [80], and *L. major* NIHS (MHOM/SN/74/Seidman, obtained from Dr. W. Robert McMaster, University of British Columbia) $\Delta gp63$ mutant and its complemented counterpart *L. major* $\Delta gp63+GP63$ [81]. Promastigotes were grown in *Leishmania* medium (M199 medium supplemented with 10% heat-inactivated fetal bovine serum [Multicell], 100 µM hypoxanthine, 10 mM HEPES, 5 µM hemin, 3 µM biotin, 1 µM biotin, penicillin [100 U/ml], and streptomycin [100 µg/ml]) at 26°C. The *L. donovani* $\Delta lpg1+LPG1$ was cultured in *Leishmania* medium supplemented with zeocin (100 µg/mL) and the *L. major* $\Delta gp63+GP63$ was cultured in *Leishmania* medium supplemented with G418 (100 µg/ml) to maintain the episomes. For infections, metacyclic promastigotes were enriched from late stationary-phase cultures using Ficoll gradients, as previously described [82]. Complement opsonization of metacyclic promastigotes and zymosan was performed prior to macrophage internalization through incubation in Hank's balanced salt solution (HBSS) containing 10% C5-deficient serum from female DBA/2 mice for 30 min at 37°C. Adherent BMM were then incubated at 37°C with metacyclic promastigotes or zymosan, and after 1h of incubation, noninternalized parasites were removed by washing three times with warm DMEM. Intracellular parasitemia was assessed at the indicated time point by counting the number of parasites per 100 infected BMM upon staining with the Hema 3 staining kit.

Antibodies

The mouse anti-VAPA monoclonal antibody (MABN361) was from Millipore, the rabbit anti-CERT polyclonal antibody (PA5-115035) was from Invitrogen, the rabbit anti-ORP1L polyclonal antibody ORP1L (ab131165), the rat anti-nSMase2 (ab85017) and the rat anti-BrdU (ab6326) were from Abcam, the rabbit anti-GLTP (10850-1-AP) was from ThermoFisher, the mouse anti-phosphoglycan (Galβ1,4Manα1-PO4) CA7AE monoclonal antibody [83] was from Cedarlane, the rabbit anti-β-actin polyclonal antibody was from Cell Signalling, and the rat LAMP-1 monoclonal antibody 1D4B developed by J.T. August and purchased through the Developmental Studies Hybridoma Bank at the University of Iowa and the National Institute of Child Health and Human Development. The secondary antibody anti-mouse conjugated to Alexa Fluor 488, and the secondary antibody anti-rabbit conjugated to Alexa Fluor 568, the secondary antibody anti-rat conjugated to Alexa Fluor 568, and the secondary antibody anti-rat conjugated to Alexa Fluor 647 used for immunofluorescence were from Invitrogen-Molecular probes.

Small interfering RNA knockdown

The protocol used for siRNA transfection was adapted from Dharmacon's cell transfection (www.dharmacon.com). BMM were seeded onto 24-well plates and reverse-transfected with

the Lipofectamine RNAiMAX Reagent (Invitrogen) as per the manufacturer's recommendation. The final concentration of siRNA was 80 nM in a final volume of 200 μ l of complete DMEM. BMM were either mock-transfected, transfected with the Non-Targeting siRNA (Dharmacon) with the following target sequence: UAGCGACUAAACACAUCAA, or transfected with the following ON-TARGET SMARTpool siRNA: Vapa (Dharmacon), which contains four siRNA with the following target sequences: sequence 1, CCAUCGGUAU GAAAAGUGU; sequence 2, CAGCCAUUUUCAUUGGAUU; sequence 3, CUACAAAUU UAAAAUUGCA; sequence 4, GUGUUUCACUCAUGAUAC; Osbp (Dharmacon) which contains four siRNA with following target sequences: sequence 1, GCGAUGAAGAUGAC GAGAA; sequence 2, AUGAAAGAGACCAGCGAAU; sequence 3, GAGAAUGGGUAUC GGUCCA; sequence 4, GAAGAGGGCUGAUCGGAGA; Col4a3bp (Dharmacon) which contains four siRNA with following target sequences: sequence 1, UCAGAGGGAAUAAAGU CGUA; sequence 2, GCGAGAAUACCCUAAGUUU; sequence 3, UCAGAGAGACGUA CUGUAU; sequence 4, GAUCACGUAUGUAGCUAAU. After 48 h cells were washed with complete medium prior to being used.

BODIPY FL-C5-Ceramide labeling and live cell microscopy

Controls and siRNA to VAPA-treated BMM seeded onto glass coverslips and infected for 48 h were washed three times with cold Hank's Balanced Salt Solution (HBSS, Invitrogen) and incubated in DMEM (without FBS) containing 0.625 μ M of BODIPYFL-C5-Ceramide (Invitrogen) for 30 min at 4°C. The cells were then washed three times with cold HBSS and incubated in DMEM without FBS at 37°C in the presence of 5% CO₂. Images of live cells were acquired in the channel 489-569 nm using a LSM780 confocal microscope (Carl Zeiss Microimaging) using X 63 objective every 5 min after the beginning of the chase.

Confocal immunofluorescence microscopy

BMM were seeded in 24-well plates containing microscope coverslips and were infected with *Leishmania* metacyclic promastigotes as described above or were fed zymosan for the indicated time points. Cells were washed with phosphate-buffered saline (PBS), fixed with 3.7% paraformaldehyde (PFA) for 30 min, and then permeabilized in 0.1% Triton X-100 for 5 min. Samples were next blocked in 10% bovine serum albumin for 1 h. Cells were incubated for 1 h the various antibodies at the following dilutions: 1:400 for the mouse anti-VAPA monoclonal antibody, 1:400 for the rabbit anti-CERT polyclonal antibody, 1:200 for the rabbit anti-ORP1L polyclonal antibody, and 1:200 for the CA7AE mouse monoclonal antibody. BMM were next incubated for 1 h with an appropriate combination of secondary antibodies (1:500 for the anti-mouse Alexa Fluor 488; 1:500 for the anti-rabbit Alexa Fluor 568, and 1:500 for the anti-IgM Alexa Fluor 568. Macrophage and promastigote nuclei were stained with DAPI (Molecular Probes). Coverslips were washed three times with PBS after every step, and individually mounted with Fluoromount-G (Invitrogen) onto slides for imaging under a confocal microscope. Analyses of distribution were performed on a LSM780 confocal microscope (Carl Zeiss Microimaging) using Plan Apochromat x 63 oil-immersion differential interference contrast (DIC) (NA 1.64) objective, and images were acquired in sequential scanning mode. Images were processed with ZEN 2012 software. At least 25 cells per condition were analyzed using the Icy image analysis software or ZEN 2012 software, and statistical differences were evaluated using one-way analysis of variance (ANOVA) followed by Tukey's posttests (three groups). Data were considered statistically significant when P was <0.05, and graphs were plotted with GraphPad Prism 5.

Proximity ligation assay

Visualization of *in situ* protein-protein interactions was carried out according to the manufacturer's protocol using Duolink *In Situ* Detection Reagents (Sigma Aldrich, DUO92004, DUO92002, DUO92008). BMM were seeded onto glass coverslips in 24-well plates and infected with *Leishmania* metacyclic promastigotes for the indicated time points. Cells were washed with phosphate-buffered saline (PBS) and fixed with 3.7% PFA for 30 min. Cells were next permeabilized with 0.2% Triton X-100. Blocking (Sigma Aldrich, DUO92004) was followed by 2 h incubation with primary antibodies directed either against VAPA (Millipore, 1:200), CERT (Invitrogen, 1:400) or ORP1L (Abcam, 1:200). After incubation the primary antibodies were washed away and PLA secondary probes were added; Anti-Rabbit MINUS (Sigma Aldrich, DUO92004, dilution 1:5), and Anti-Mouse PLUS (Sigma Aldrich, DUO92002, dilution 1:5) following by 1 h incubation in a humidified chamber at 37°C. The coverslips were twice washed in Duolink *In situ* wash buffer A for 5 min under gentle agitation. Ligation was then done by adding Ligation buffer (Sigma Aldrich, dilution 1:5) and Ligase (Sigma Aldrich, dilution 1:40) solutions to each sample and for 30 min incubation in a humidified chamber at 37°C. The coverslips were then washed twice in 1X Duolink *In Situ* wash buffer A for 2 min under gentle agitation, and then placed in amplification buffer (Sigma Aldrich, DUO92008, dilution 1:80) solution and incubated 100 min at 37°C, followed by washing twice in 1X wash buffer B (Sigma Aldrich) and then once for 1 min in 100 X diluted wash buffer B, and drying at room temperature in the dark. Coverslips were incubated for additional 10 min with DAPI and then individually mounted with Fluoromount-G (Invitrogen, ref.00-4958-02) onto slides. Analyses were performed on a LSM780 confocal microscope (Carl Zeiss Microimaging) using Plan Apochromat X 63 oil-immersion differential interference contrast (DIC). To determine the background PLA signal, the same procedures were followed as described above except that the cell-containing coverslips were incubated with only one of the individual primary antibodies. Images of PLA are visualized as red dots and were analyzed with Zen software by manual counting. The imaging results are presented as the mean of the three trial values \pm standard deviation. Statistical significance (*p*-values) was determined using a one-way ANOVA test in the software GraphPad Prism 5.

BrdU labeling

BMM were seeded in 24-well plates containing microscope coverslips and were infected with *Leishmania* metacyclic. Two hours after parasites were added, BMM were washed three times to remove extracellular parasites, placed in media containing 0.1 mM BrdU (Sigma), and were incubated for various time points after phagocytosis. Cells were fixed with 3.7% PFA for 30 min, permeabilized in 0.1% Triton X-100 for 5 min, and were stained with a rat anti-BrdU monoclonal antibody [43].

Western blot analyses

Prior to lysis, adherent BMMs were placed on ice and washed 3 times with PBS containing 1 mM sodium orthovanadate and 5 mM 1,10-phenanthroline [49]. Cells were scraped in the presence of lysis buffer containing 1% NP-40, 50 mM Tris-HCl (pH 7.5), 150 mM NaCl, 1 mM EDTA (pH 8), 10 mM 1,10-phenanthroline, and phosphatase and protease inhibitors (Roche) [49]. After 24 h incubation at -20°C, lysates were centrifuged for 30 min, and the soluble phase was collected. After protein quantification, 25 μ g of protein was boiled (100°C) for 5 min in SDS sample buffer and migrated in SDS-PAGE gels. Proteins were transferred onto Hybond-ECL membranes (Amersham Biosciences), blocked for 1 h in Tris-buffered saline (TBS) 1 \times 0.1% Tween containing 5% BSA, and incubated with primary antibodies (diluted in TBS 1 \times

0.1% Tween containing 5% BSA) overnight at 4°C and then with appropriate horseradish peroxidase (HRP)-conjugated secondary antibodies for 1 h at room temperature. Membranes were incubated in ECL (GE Healthcare), and immunodetection was achieved via chemiluminescence using the Azure Biosystem.

Statistics and reproducibility

GraphPad Prism 5 software was used to generate the graphs and statistical analyses. All experiments were conducted three independent times. Methods for statistical tests, exact value of n , and definition of error bars are indicated in the figure legends; *, $P < 0.05$; **, $P < 0.01$; ***, $P < 0.001$. All immunoblots and images shown are representative of these independent experiments.

Supporting information

S1 Fig. Efficacy of siRNA-mediated knockdown of VAPA in BMM. Representative Western blots of VAPA levels in untreated BMM (unt), BMM treated with scrambled siRNA (siScr), mock transfected BMM (mock) and BMM treated with siRNA to VAPA (siVAPA). Levels of β -actin were used as controls. Blots for the levels of VAPA for the results shown in Figs 2A-E, 3A, 3B and 6B.
(TIFF)

S2 Fig. Efficacy of siRNA-mediated knockdown of CERT and ORP1L in BMM. Representative Western blots of CERT and ORP1L levels in untreated BMM (unt), BMM treated with scrambled siRNA (siScr), mock transfected BMM (mock) and BMM treated with either siRNA to CERT (siCERT) or siRNA to ORP1L (siOSBP). Levels of β -actin were used as controls. Blots for the levels of CERT for the results shown in Fig 4D and 4F and in for the levels of ORP1L for the results shown in Fig 4E and 4G.
(TIFF)

S3 Fig. Controls for the proximity ligation assays. (A) To determine the background signal of proximity ligation assays, adherent BMM were incubated with only one of the individual primary antibodies at a time. Proximity ligation assays were performed on uninfected BMM in the absence of the secondary antibodies against either the anti-rabbit primary antibodies or the anti-mouse primary antibodies. (B). Positive control for the proximity ligation assays was performed on uninfected BMM using primary antibodies against ORP1L and VAPA. Red dots represent VAPA-ORP1L *in situ* complexes. DNA is in blue.
(TIFF)

S4 Fig. Disruption of VAPA-GLTP *in situ* complexes by *L. amazonensis*. (A) BMMs were infected or not with either *L. amazonensis* metacyclic promastigotes. At 24 h post-infection, VAPA-GLTP *in situ* complexes were detected by proximity ligation and visualized by confocal immunofluorescence microscopy (red dots). DNA is in blue. (B) Quantification of *in situ* complexes for VAPA-GLTP in uninfected BMM and in BMM infected with *L. amazonensis*. Data are presented as clouds with means \pm standard deviations (SD) of values from three independent experiments for a total of 75 cells in each group. ***, $P \leq 0.01$.
(TIFF)

S1 Data. Source data for Figs 1B, 2A, 2B, 2D-E, 3B, 4D-G, 5B, 5D, 5E, 5F and S4B.
(XLSX)

Acknowledgments

We thank Dr Laurent Chatel-Chaix and Dr Olus Uyar for advice with proximity ligation assays, Dr Hamlet Acevedo Ospina for thoughtful comments on this manuscript, and Mr. Jessy Tremblay for expert assistance in immunofluorescence confocal microscopy experiments.

Author contributions

Conceptualization: Ilona Gdovinova, Albert Descoteaux.

Data curation: Ilona Gdovinova, Albert Descoteaux.

Formal analysis: Ilona Gdovinova, Albert Descoteaux.

Funding acquisition: Albert Descoteaux.

Investigation: Ilona Gdovinova.

Methodology: Ilona Gdovinova, Albert Descoteaux.

Project administration: Albert Descoteaux.

Resources: Albert Descoteaux.

Supervision: Albert Descoteaux.

Visualization: Ilona Gdovinova, Albert Descoteaux.

Writing – original draft: Ilona Gdovinova, Albert Descoteaux.

Writing – review & editing: Albert Descoteaux.

References

1. Herwaldt BL. Leishmaniasis. *Lancet*. 1999;354(9185):1191–9.
2. Desjardins M, Descoteaux A. Inhibition of phagolysosomal biogenesis by the *Leishmania* lipophosphoglycan. *J Exp Med*. 1997;185(12):2061–8. <https://doi.org/10.1084/jem.185.12.2061> PMID: 9182677
3. Holm A, Tejle K, Magnusson KE, Descoteaux A, Rasmussen B. *Leishmania donovani* lipophosphoglycan causes periphagosomal actin accumulation: correlation with impaired translocation of PKC α and defective phagosome maturation. *Cell Microbiol*. 2001;3(7):439–47. <https://doi.org/10.1046/j.1462-5822.2001.00127.x> PMID: 11437830
4. Lodge R, Diallo TO, Descoteaux A. *Leishmania donovani* lipophosphoglycan blocks NADPH oxidase assembly at the phagosome membrane. *Cell Microbiol*. 2006;8(12):1922–31. <https://doi.org/10.1111/j.1462-5822.2006.00758.x> PMID: 16848789
5. Scianimanico S, Desrosiers M, Dermine JF, Méresse S, Descoteaux A, Desjardins M. Impaired recruitment of the small GTPase rab7 correlates with the inhibition of phagosome maturation by *Leishmania donovani* promastigotes. *Cell Microbiol*. 1999;1(1):19–32. <https://doi.org/10.1046/j.1462-5822.1999.00002.x> PMID: 11207538
6. Arango Duque G, Fukuda M, Turco SJ, Stäger S, Descoteaux A. *Leishmania* promastigotes induce cytokine secretion in macrophages through the degradation of synaptotagmin XI. *J Immunol*. 2014;193(5):2363–72. <https://doi.org/10.4049/jimmunol.1303043> PMID: 25063865
7. Vinet AF, Fukuda M, Turco SJ, Descoteaux A. The *Leishmania donovani* lipophosphoglycan excludes the vesicular proton-ATPase from phagosomes by impairing the recruitment of synaptotagmin V. *PLoS Pathog*. 2009;5(10):e1000628. <https://doi.org/10.1371/journal.ppat.1000628> PMID: 19834555
8. Dermine JF, Scianimanico S, Privé C, Descoteaux A, Desjardins M. *Leishmania* promastigotes require lipophosphoglycan to actively modulate the fusion properties of phagosomes at an early step of phagocytosis. *Cell Microbiol*. 2000;2(2):115–26. <https://doi.org/10.1046/j.1462-5822.2000.00037.x> PMID: 11207568
9. Batista MF, Nájera CA, Meneghelli I, Bahia D. The Parasitic Intracellular Lifestyle of Trypanosomatids: Parasitophorous Vacuole Development and Survival. *Front Cell Dev Biol*. 2020;8:396. <https://doi.org/10.3389/fcell.2020.00396> PMID: 32587854
10. Séguin O, Mai LT, Acevedo Ospina H, Guay-Vincent M-M, Whiteheart SW, Stäger S, et al. VAMP3 and VAMP8 Regulate the Development and Functionality of Parasitophorous Vacuoles Housing

- Leishmania amazonensis*. Infect Immun. 2022;90(3):e0018321. <https://doi.org/10.1128/IAI.00183-21> PMID: [35130453](https://pubmed.ncbi.nlm.nih.gov/35130453/)
11. Matheoud D, Moradin N, Bellemare-Pelletier A, Shio MT, Hong WJ, Olivier M, et al. *Leishmania* evades host immunity by inhibiting antigen cross-presentation through direct cleavage of the SNARE VAMP8. Cell Host Microbe. 2013;14(1):15–25. <https://doi.org/10.1016/j.chom.2013.06.003> PMID: [23870310](https://pubmed.ncbi.nlm.nih.gov/23870310/)
 12. Matte C, Casgrain P-A, Séguin O, Moradin N, Hong WJ, Descoteaux A. *Leishmania* major Promastigotes Evade LC3-Associated Phagocytosis through the Action of GP63. PLoS Pathog. 2016;12(6):e1005690. <https://doi.org/10.1371/journal.ppat.1005690> PMID: [27280768](https://pubmed.ncbi.nlm.nih.gov/27280768/)
 13. Matte C, Descoteaux A. Exploitation of the Host Cell Membrane Fusion Machinery by *Leishmania* Is Part of the Infection Process. PLoS Pathog. 2016;12(12):e1005962. <https://doi.org/10.1371/journal.ppat.1005962> PMID: [27930749](https://pubmed.ncbi.nlm.nih.gov/27930749/)
 14. Canton J, Kima P. Targeting host syntaxin-5 preferentially blocks *Leishmania* parasitophorous vacuole development in infected cells and limits experimental *Leishmania* infections. American Journal of Pathology. 2012;181(4):1348–55.
 15. Canton J, Ndjamen B, Hatsuzawa K, Kima PE. Disruption of the fusion of *Leishmania* parasitophorous vacuoles with ER vesicles results in the control of the infection. Cell Microbiol. 2012;14(6):937–48.
 16. Boggild AK, Caumes E, Grobusch MP, Schwartz E, Hynes NA, Libman M, et al. Cutaneous and mucocutaneous leishmaniasis in travellers and migrants: a 20-year GeoSentinel Surveillance Network analysis. J Travel Med. 2019;26(8):taz055. <https://doi.org/10.1093/jtm/taz055> PMID: [31553455](https://pubmed.ncbi.nlm.nih.gov/31553455/)
 17. Kima PE, Bonilla JA, Cho E, Ndjamen B, Canton J, Leal N, et al. Identification of *Leishmania* proteins preferentially released in infected cells using change mediated antigen technology (CMAT). PLoS Negl Trop Dis. 2010;4(10):e842. <https://doi.org/10.1371/journal.pntd.0000842> PMID: [20957202](https://pubmed.ncbi.nlm.nih.gov/20957202/)
 18. McConville MJ, de Souza D, Saunders E, Likic VA, Naderer T. Living in a phagolysosome; metabolism of *Leishmania* amastigotes. 2007. p. 368–75.
 19. McConville MJ, Naderer T. Metabolic pathways required for the intracellular survival of *Leishmania*. Annual Review of Microbiology. 2011;65:543–61.
 20. Laranjeira-Silva MF, Hamza I, Pérez-Victoria JM. Iron and Heme Metabolism at the *Leishmania*-Host Interface. Trends Parasitol. 2020;36(3):279–89. <https://doi.org/10.1016/j.pt.2019.12.010> PMID: [32005611](https://pubmed.ncbi.nlm.nih.gov/32005611/)
 21. Zhang K, Beverley SM. Phospholipid and sphingolipid metabolism in *Leishmania*. Mol Biochem Parasitol. 2010;170(2):55–64. <https://doi.org/10.1016/j.molbiopara.2009.12.004> PMID: [20026359](https://pubmed.ncbi.nlm.nih.gov/20026359/)
 22. Zhang K, Bangs JD, Beverley SM. Sphingolipids in parasitic protozoa. Adv Exp Med Biol. 2010;688:238–48. https://doi.org/10.1007/978-1-4419-6741-1_17 PMID: [20919659](https://pubmed.ncbi.nlm.nih.gov/20919659/)
 23. Zhang K. Balancing de novo synthesis and salvage of lipids by *Leishmania* amastigotes. Curr Opin Microbiol. 2021;63:98–103. <https://doi.org/10.1016/j.mib.2021.07.004> PMID: [34311265](https://pubmed.ncbi.nlm.nih.gov/34311265/)
 24. Denny PW, Goulding D, Ferguson MAJ, Smith DF. Sphingolipid-free *Leishmania* are defective in membrane trafficking, differentiation and infectivity. Mol Microbiol. 2004;52(2):313–27. <https://doi.org/10.1111/j.1365-2958.2003.03975.x> PMID: [15066023](https://pubmed.ncbi.nlm.nih.gov/15066023/)
 25. Kuhlmann F, Key P, Hickerson S, Turk J, Hsu F, Beverley S. Inositol phosphorylceramide synthase null *Leishmania* are viable and virulent in animal infections where salvage of host sphingomyelin predominates. J Biol Chem. 2022;298(11):102522. <https://doi.org/10.1016/j.jbc.2022.102522>
 26. Zhang K, Hsu F-F, Scott DA, Docampo R, Turk J, Beverley SM. *Leishmania* salvage and remodeling of host sphingolipids in amastigote survival and acidocalcisome biogenesis. Mol Microbiol. 2005;55(5):1566–78. <https://doi.org/10.1111/j.1365-2958.2005.04493.x> PMID: [15720561](https://pubmed.ncbi.nlm.nih.gov/15720561/)
 27. Backman APE, Mattjus P. Who moves the sphinx? An overview of intracellular sphingolipid transport. Biochim Biophys Acta Mol Cell Biol Lipids. 2021;1866(11):159021. <https://doi.org/10.1016/j.bbalip.2021.159021> PMID: [34339859](https://pubmed.ncbi.nlm.nih.gov/34339859/)
 28. Hoekstra D, Kok JW. Trafficking of glycosphingolipids in eukaryotic cells; sorting and recycling of lipids. Biochim Biophys Acta. 1992;1113(3–4):277–94. [https://doi.org/10.1016/0304-4157\(92\)90002-r](https://doi.org/10.1016/0304-4157(92)90002-r) PMID: [1450202](https://pubmed.ncbi.nlm.nih.gov/1450202/)
 29. Kawano M, Kumagai K, Nishijima M, Hanada K. Efficient trafficking of ceramide from the endoplasmic reticulum to the Golgi apparatus requires a VAMP-associated protein-interacting FFAT motif of CERT. J Biol Chem. 2006;281(40):30279–88. <https://doi.org/10.1074/jbc.M605032200> PMID: [16895911](https://pubmed.ncbi.nlm.nih.gov/16895911/)
 30. Cohen S, Valm AM, Lippincott-Schwartz J. Interacting organelles. Curr Opin Cell Biol. 2018;53:84–91. <https://doi.org/10.1016/j.ceb.2018.06.003> PMID: [30006038](https://pubmed.ncbi.nlm.nih.gov/30006038/)

31. Kors S, Costello JL, Schrader M. VAP Proteins - From Organelle Tethers to Pathogenic Host Interactors and Their Role in Neuronal Disease. *Front Cell Dev Biol.* 2022;10:895856. <https://doi.org/10.3389/fcell.2022.895856> PMID: [35756994](https://pubmed.ncbi.nlm.nih.gov/35756994/)
32. Voeltz GK, Sawyer EM, Hajnóczky G, Prinz WA. Making the connection: How membrane contact sites have changed our view of organelle biology. *Cell.* 2024;187(2):257–70. <https://doi.org/10.1016/j.cell.2023.11.040> PMID: [38242082](https://pubmed.ncbi.nlm.nih.gov/38242082/)
33. Vormittag S, Ende RJ, Derré I, Hilbi H. Pathogen vacuole membrane contact sites - close encounters of the fifth kind. *Microlife.* 2023;4:uqad018. <https://doi.org/10.1093/femsml/uqad018> PMID: [37223745](https://pubmed.ncbi.nlm.nih.gov/37223745/)
34. Nunes-Hasler P, Demaurex N. The ER phagosome connection in the era of membrane contact sites. *Biochim Biophys Acta Mol Cell Res.* 2017;1864(9):1513–24. <https://doi.org/10.1016/j.bbamcr.2017.04.007> PMID: [28432021](https://pubmed.ncbi.nlm.nih.gov/28432021/)
35. Derré I. Hijacking of Membrane Contact Sites by Intracellular Bacterial Pathogens. *Adv Exp Med Biol.* 2017;997:211–23. https://doi.org/10.1007/978-981-10-4567-7_16 PMID: [28815533](https://pubmed.ncbi.nlm.nih.gov/28815533/)
36. Paul P, Tiwari B. Organelles are miscommunicating: Membrane contact sites getting hijacked by pathogens. *Virulence.* 2023;14(1):2265095. <https://doi.org/10.1080/21505594.2023.2265095> PMID: [37862470](https://pubmed.ncbi.nlm.nih.gov/37862470/)
37. Derré I, Swiss R, Agaisse H. The lipid transfer protein CERT interacts with the Chlamydia inclusion protein IncD and participates to ER-Chlamydia inclusion membrane contact sites. *PLoS Pathog.* 2011;7(6):e1002092. <https://doi.org/10.1371/journal.ppat.1002092> PMID: [21731489](https://pubmed.ncbi.nlm.nih.gov/21731489/)
38. Elwell CA, Jiang S, Kim JH, Lee A, Wittmann T, Hanada K, et al. Chlamydia trachomatis co-opts GBF1 and CERT to acquire host sphingomyelin for distinct roles during intracellular development. *PLoS Pathog.* 2011;7(9):e1002198. <https://doi.org/10.1371/journal.ppat.1002198> PMID: [21909260](https://pubmed.ncbi.nlm.nih.gov/21909260/)
39. Murray R, Flora E, Bayne C, Derré I. IncV, a FFAT motif-containing Chlamydia protein, tethers the endoplasmic reticulum to the pathogen-containing vacuole. *Proc Natl Acad Sci U S A.* 2017;114(45):12039–44. <https://doi.org/10.1073/pnas.1709060114> PMID: [29078338](https://pubmed.ncbi.nlm.nih.gov/29078338/)
40. Subtil A. Rerouting of host lipids by bacteria: are you CERTain you need a vesicle?. *PLoS Pathog.* 2011;7(9):e1002208. <https://doi.org/10.1371/journal.ppat.1002208> PMID: [21909265](https://pubmed.ncbi.nlm.nih.gov/21909265/)
41. Ndjamien B, Kang B-H, Hatsuzawa K, Kima PE. Leishmania parasitophorous vacuoles interact continuously with the host cell's endoplasmic reticulum; parasitophorous vacuoles are hybrid compartments. *Cell Microbiol.* 2010;12(10):1480–94. <https://doi.org/10.1111/j.1462-5822.2010.01483.x> PMID: [20497181](https://pubmed.ncbi.nlm.nih.gov/20497181/)
42. Neefjes J, Cabukusta B. What the VAP: The Expanded VAP Family of Proteins Interacting With FFAT and FFAT-Related Motifs for Interorganellar Contact. *Contact (Thousand Oaks).* 2021;4:25152564211012246. <https://doi.org/10.1177/25152564211012246> PMID: [34036242](https://pubmed.ncbi.nlm.nih.gov/34036242/)
43. Mandell MA, Beverley SM. Continual renewal and replication of persistent *Leishmania major* parasites in concomitantly immune hosts. *Proc Natl Acad Sci U S A.* 2017;114(5):E801–10. <https://doi.org/10.1073/pnas.1619265114> PMID: [28096392](https://pubmed.ncbi.nlm.nih.gov/28096392/)
44. James C, Kehlenbach RH. The interactome of the VAP Family of Proteins: An Overview. *Cells.* 2021;10(7):1780. <https://doi.org/10.3390/cells10071780> PMID: [34359948](https://pubmed.ncbi.nlm.nih.gov/34359948/)
45. Subra M, Antonny B, Mesmin B. New insights into the OSBP–VAP cycle. *Curr Opin Cell Biol.* 2023;82:102172. <https://doi.org/10.1016/j.ceb.2023.102172> PMID: [37245352](https://pubmed.ncbi.nlm.nih.gov/37245352/)
46. Barman B, Sung BH, Krystofiak E, Ping J, Ramirez M, Millis B, et al. VAP-A and its binding partner CERT drive biogenesis of RNA-containing extracellular vesicles at ER membrane contact sites. *Dev Cell.* 2022;57(8):974–994.e8. <https://doi.org/10.1016/j.devcel.2022.03.012> PMID: [35421371](https://pubmed.ncbi.nlm.nih.gov/35421371/)
47. Dermine J-F, Goyette G, Houde M, Turco SJ, Desjardins M. *Leishmania donovani* lipophosphoglycan disrupts phagosome microdomains in J774 macrophages. *Cell Microbiol.* 2005;7(9):1263–70. <https://doi.org/10.1111/j.1462-5822.2005.00550.x> PMID: [16098214](https://pubmed.ncbi.nlm.nih.gov/16098214/)
48. Winberg ME, Holm A, Särndahl E, Vinet AF, Descoteaux A, Magnusson K-E, et al. *Leishmania donovani* lipophosphoglycan inhibits phagosomal maturation via action on membrane rafts. *Microbes Infect.* 2009;11(2):215–22. <https://doi.org/10.1016/j.micinf.2008.11.007> PMID: [19070677](https://pubmed.ncbi.nlm.nih.gov/19070677/)
49. Guay-Vincent M-M, Matte C, Berthiaume A-M, Olivier M, Jaramillo M, Descoteaux A. Revisiting *Leishmania* GP63 host cell targets reveals a limited spectrum of substrates. *PLoS Pathog.* 2022;18(10):e1010640. <https://doi.org/10.1371/journal.ppat.1010640> PMID: [36191034](https://pubmed.ncbi.nlm.nih.gov/36191034/)
50. Turco SJ, Descoteaux A. The lipophosphoglycan of *Leishmania* parasites. *Annu Rev Microbiol.* 1992;46:65–94. <https://doi.org/10.1146/annurev.mi.46.100192.000433> PMID: [1444269](https://pubmed.ncbi.nlm.nih.gov/1444269/)

51. Arango Duque G, Jardim A, Gagnon É, Fukuda M, Descoteaux A. The host cell secretory pathway mediates the export of *Leishmania* virulence factors out of the parasitophorous vacuole. *PLoS Pathog.* 2019;15(7):e1007982. <https://doi.org/10.1371/journal.ppat.1007982> PMID: 31356625
52. Jackson CL, Walch L, Verbavatz JM. Lipids and their trafficking: An integral part of cellular organization. *Developmental Cell.* 2016;39(2):139–53.
53. Phillips MJ, Voeltz GK. Structure and function of ER membrane contact sites with other organelles. *Nat Rev Mol Cell Biol.* 2016;17(2):69–82. <https://doi.org/10.1038/nrm.2015.8> PMID: 26627931
54. Wu H, Carvalho P, Voeltz GK. Here, there, and everywhere: The importance of ER membrane contact sites. *Science.* 2018;361(6401):eaan5835. <https://doi.org/10.1126/science.aan5835> PMID: 30072511
55. Pessoa CC, Reis LC, Ramos-Sanchez EM, Orikaza CM, Cortez C, de Castro Levatti EV, et al. ATP6V0d2 controls *Leishmania* parasitophorous vacuole biogenesis via cholesterol homeostasis. *PLoS Pathog.* 2019;15(6):e1007834. <https://doi.org/10.1371/journal.ppat.1007834> PMID: 31199856
56. Chen Y, Zhang J, Cui W, Silverstein R. CD36, a signaling receptor and fatty acid transporter that regulates immune cell metabolism and fate. *J Exp Med.* 2022;219(6).
57. Okuda K, Tong M, Dempsey B, Moore KJ, Gazzinelli RT, Silverman N. *Leishmania amazonensis* Engages CD36 to Drive Parasitophorous Vacuole Maturation. *PLoS Pathog.* 2016;12(6):e1005669. <https://doi.org/10.1371/journal.ppat.1005669> PMID: 27280707
58. Rabhi I, Rabhi S, Ben-Othman R, Rasche A, Daskalaki A, Trentin B, et al. Transcriptomic signature of *Leishmania* infected mice macrophages: a metabolic point of view. *PLoS Negl Trop Dis.* 2012;6(8):e1763. <https://doi.org/10.1371/journal.pntd.0001763> PMID: 22928052
59. Rabhi S, Rabhi I, Trentin B, Piquemal D, Regnault B, Goyard S, et al. Lipid Droplet Formation, Their Localization and Dynamics during *Leishmania* major Macrophage Infection. *PLoS One.* 2016;11(2):e0148640. <https://doi.org/10.1371/journal.pone.0148640> PMID: 26871576
60. Sood C, Verma JK, Basak R, Kapoor A, Gupta S, Mukhopadhyay A. *Leishmania* hijack host lipid body for its proliferation in macrophages by overexpressing host Rab18 and TRAPPC9 by downregulating miR-1914-3p expression. *PLoS Pathog.* 2024;20(2):e1012024. <https://doi.org/10.1371/journal.ppat.1012024> PMID: 38412149
61. Zhang O, Wilson MC, Xu W, Hsu F-F, Turk J, Kuhlmann FM, et al. Degradation of host sphingomyelin is essential for *Leishmania* virulence. *PLoS Pathog.* 2009;5(12):e1000692. <https://doi.org/10.1371/journal.ppat.1000692> PMID: 20011126
62. Xu W, Xin L, Soong L, Zhang K. Sphingolipid degradation by *Leishmania* major is required for its resistance to acidic pH in the mammalian host. *Infection and Immunity.* 2011;79(8):3377–87.
63. Hannun YA, Obeid LM. Sphingolipids and their metabolism in physiology and disease. *Nat Rev Mol Cell Biol.* 2018;19(3):175–91. <https://doi.org/10.1038/nrm.2017.107> PMID: 29165427
64. Sacks DL. *Leishmania*-sand fly interactions controlling species-specific vector competence. *Cell Microbiol.* 2001;3(4):189–96.
65. Sacks D, Kamhawi S. Molecular aspects of parasite-vector and vector-host interactions in leishmaniasis. *Annu Rev Microbiol.* 2001;55:453–83. <https://doi.org/10.1146/annurev.micro.55.1.453> PMID: 11544364
66. Moradin N, Descoteaux A. *Leishmania* promastigotes: building a safe niche within macrophages. *Frontiers in Cellular and Infection Microbiology.* 2012;2:121.
67. Descoteaux A, Turco SJ, Sacks DL, Matlashewski G. *Leishmania donovani* lipophosphoglycan selectively inhibits signal transduction in macrophages. *J Immunol.* 1991;146(8):2747–53. <https://doi.org/10.4049/jimmunol.146.8.2747> PMID: 1707920
68. Descoteaux A, Matlashewski G, Turco SJ. Inhibition of macrophage protein kinase C-mediated protein phosphorylation by *Leishmania donovani* lipophosphoglycan. *J Immunol.* 1992;149(9):3008–15. <https://doi.org/10.4049/jimmunol.149.9.3008> PMID: 1383336
69. de Carvalho RVH, Andrade WA, Lima-Junior DS, Dilucca M, de Oliveira CV, Wang K, et al. *Leishmania* Lipophosphoglycan Triggers Caspase-11 and the Non-canonical Activation of the NLRP3 Inflammasome. *Cell Rep.* 2019;26(2):429–437.e5. <https://doi.org/10.1016/j.celrep.2018.12.047> PMID: 30625325
70. Acevedo Ospina H, Guay-Vincent M-M, Descoteaux A. Macrophage Mitochondrial Biogenesis and Metabolic Reprogramming Induced by *Leishmania donovani* Require Lipophosphoglycan and Type I Interferon Signaling. *mBio.* 2022;13(6):e0257822. <https://doi.org/10.1128/mbio.02578-22> PMID: 36222510
71. Weir ML, Xie H, Klip A, Trimble WS. VAP-A binds promiscuously to both v- and tSNAREs. *Biochem Biophys Res Commun.* 2001;286(3):616–21. <https://doi.org/10.1006/bbrc.2001.5437> PMID: 11511104

72. Petkovic M, Jemaiei A, Daste F, Specht CG, Izeddin I, Vorkel D, et al. The SNARE Sec22b has a non-fusogenic function in plasma membrane expansion. *Nat Cell Biol.* 2014;16(5):434–44. <https://doi.org/10.1038/ncb2937> PMID: [24705552](https://pubmed.ncbi.nlm.nih.gov/24705552/)
73. Criado Santos N, Bouvet S, Cruz Cobo M, Mandavit M, Bermont F, Castelbou C. Sec22b regulates phagosome maturation by promoting ORP8-mediated lipid exchange at endoplasmic reticulum-phagosome contact sites. *Commun Biol.* 2023;6(1):1008.
74. Menu P, Mayor A, Zhou R, Tardivel A, Ichijo H, Mori K, et al. ER stress activates the NLRP3 inflammasome via an UPR-independent pathway. *Cell Death Dis.* 2012;3(1):e261. <https://doi.org/10.1038/cddis.2011.132> PMID: [22278288](https://pubmed.ncbi.nlm.nih.gov/22278288/)
75. Dias-Teixeira KL, Pereira RM, Silva JS, Fasel N, Aktas BH, Lopes UG. Unveiling the Role of the Integrated Endoplasmic Reticulum Stress Response in Leishmania Infection - Future Perspectives. *Front Immunol.* 2016;7:283. <https://doi.org/10.3389/fimmu.2016.00283> PMID: [27499755](https://pubmed.ncbi.nlm.nih.gov/27499755/)
76. McConville M, Ralton J. Developmentally regulated changes in the cell surface architecture of Leishmania parasites. *Behring Institute Mitteilungen.* 1997;1997(99):34–43.
77. Descoteaux A, Turco SJ. Glycoconjugates in Leishmania infectivity. *Biochim Biophys Acta.* 1999;1455(2–3):341–52. [https://doi.org/10.1016/s0925-4439\(99\)00065-4](https://doi.org/10.1016/s0925-4439(99)00065-4) PMID: [10571023](https://pubmed.ncbi.nlm.nih.gov/10571023/)
78. Yang S-T, Kreutzberger AJB, Lee J, Kiessling V, Tamm LK. The role of cholesterol in membrane fusion. *Chem Phys Lipids.* 2016;199:136–43. <https://doi.org/10.1016/j.chemphyslip.2016.05.003> PMID: [27179407](https://pubmed.ncbi.nlm.nih.gov/27179407/)
79. Radulovic M, Wenzel EM, Gilani S, Holland LK, Lystad AH, Phuyal S, et al. Cholesterol transfer via endoplasmic reticulum contacts mediates lysosome damage repair. *EMBO J.* 2022;41(24):e112677. <https://doi.org/10.15252/embj.2022112677> PMID: [36408828](https://pubmed.ncbi.nlm.nih.gov/36408828/)
80. Matte C, Arango Duque G, Descoteaux A. Leishmania donovani Metacyclic Promastigotes Impair Phagosome Properties in Inflammatory Monocytes. *Infect Immun.* 2021;89(7):e0000921. <https://doi.org/10.1128/IAI.00009-21> PMID: [33875473](https://pubmed.ncbi.nlm.nih.gov/33875473/)
81. Joshi P, Kelly B, Kamhawi S, Sacks D, McMaster W. Targeted gene deletion in Leishmania major identifies leishmanolysin (GP63) as a virulence factor. *Molecular and Biochemical Parasitology.* 2002;120(1):33–40.
82. Späth GF, Beverley SM. A lipophosphoglycan-independent method for isolation of infective Leishmania metacyclic promastigotes by density gradient centrifugation. *Exp Parasitol.* 2001;99(2):97–103. <https://doi.org/10.1006/expr.2001.4656> PMID: [11748963](https://pubmed.ncbi.nlm.nih.gov/11748963/)
83. Tolson DL, Turco SJ, Pearson TW. Expression of a repeating phosphorylated disaccharide lipophosphoglycan epitope on the surface of macrophages infected with Leishmania donovani. *Infection and Immunity.* 1990;58(11):3500–7.